Metal-Directed Self-Assembly: Two New Metal-Binicotinate Grid Polymeric Networks and Their Fluorescence Emission Tuned by Ligand Configuration

Benlai Wu,[a] Daqiang Yuan,[a] Feilong Jiang,[a] Ruihu Wang,[a] Lei Han,[a] Youfu Zhou,[a] and Maochun Hong*[a]

Keywords: Self-assembly / Binicotinic acid / Fluorescence / Coordination polymer / Chirality

Two new 2-D metal-binicotinate coordination polymers, namely, $[Cd^{II}(bpdc)]_n$ (**1**) and $\{[Zn^{II}_8(bpdc)_8(H_2O)_8](H_2O)_8\}_n$ (**2**) (H_2bpdc = binicotinic acid) have been synthesized using hydrothermal and three-layer diffusion methods, respectively. Single-crystal X-ray analyses revealed that both are extended grid networks of the (4,4) topology. Their structures alter with the configuration and function of bpdc. The achiral, free H_2bpdc has axial chirality induced by metal coordination in **1**, and bpdc connects to four metal centers forming a 2-D (4,4) net with three kinds of apertures generated through self-assembly. In **2**, however, bpdc connects to three metal centers, fabricating a microporous framework containing hydrophilic channels. Studies on the solid emission spectra of the free ligand, **1**, and **2** confirmed, that the configuration of bpdc resulting from metal-directed coordination has a profound effect on the fluorescence emissions of **1** and **2**.

Introduction

The construction of extended metal-organic networks, especially with micropores, is of current interest in the fields of supramolecular chemistry and crystal engineering, because of their exploitable magnetic,[1−3] catalytic,[4] optoelectronic,[5,6] and inclusive properties.[7] The self-assembly of suitable ligands and metal centers has been proved to be an efficient route for the formation of one- to three-dimensional networks with fascinating structural topologies.[8−11]

Recently, interest has increasingly been centered on self-assembly of metal ions with multi-pyridine and multi-carboxylate spacers.[12−15] As exemplified by the successful syntheses of porous networks, the rigid skeletons of multi-pyridine ligands always sustain the frameworks, and the diversely coordinating multi-carboxylate spacers can help enhance the stability of the resultant metal-organic networks.[16,17] The family of binicotinic acid ligands (H_2bpdc) bearing 2,2′-bipyridyl and dicarboxyl functional groups has received considerable attention in photochemistry and crystal engineering.[18−25] On the one hand, owing to the structural features of the strong chelating bipyridyl moiety and the adjacent carboxyl groups, these ligands often acts as bis(monodentate),[18] tridentate[19,20] or bis(bidentate)[20,21] bridging spacers, and facilitate the formation of 1-D catenopolymers, indicating ligand-directed synthesis. On the other hand, the configuration of bpdc can be greatly altered along the 1,1′ bond, while the pyridyl and carboxyl functional groups bind to the selected metal centers. This may also provide a route for metal-directed synthesis, something which has been rarely reported in the literature. In this work we selected Cd^{II} and Zn^{II} as metal nodes for assembly with Me_2bpdc (dimethyl 2,2′-bipyridine-3,3′-dicarboxylate) and H_2bpdc, respectively, and obtained two 2-D novel coordination polymers, namely, $[Cd^{II}(bpdc)]_n$ (**1**) and $\{[Zn^{II}_8(bpdc)_8(H_2O)_8](H_2O)_8\}_n$ (**2**). Complex **1**, which was assembled under hydrothermal conditions, has a (4,4) topological network with three-shaped apertures, while complex **2**, obtained through a three-layer diffusion method, exhibits a microporous framework containing hydrophilic channels.

We also report the interesting results of fluorescence emission experiments, which show that the configuration of bpdc resulting from metal-directed coordination has a profound effect on the emissions of **1** and **2**.

Results and Discussion

Using hydrothermal methods, the crystalline complex **1** was successfully obtained through the reaction of Me_2bpdc with $CdCl_2{\cdot}2.5H_2O$ (ratio 1:1) in the presence of triethylamine at 160 °C, under which conditions Me_2bpdc underwent hydrolytic decomposition to give bpdc. Substituting $CdCl_2{\cdot}2.5H_2O$ with $ZnCl_2$ under the same reaction conditions yielded only a white precipitate. Finally, single crys-

[a] State Key Laboratory of Structural Chemistry, Fujian Institute of the Research on the Structure of Matter, Chinese Academy of Sciences,
Fuzhou, Fujian, 350002, China
Fax: (internat.) + 86-591-371-4946
E-mail: hmc@ms.fjirsm.ac.cn

Supporting information for this article is available on the WWW under http://www.eurjic.org or from the author.

tals of compound **2** were obtained in a three-layer diffusion system with a aqueous solution of H_2bpdc as the bottom layer, a mixture of DMF, water, and methanol as the mesosphere, and a methanol solution of $ZnCl_2$ as the top layer.

Structural Description

A single-crystal X-ray diffraction analysis revealed, that complex **1** crystallizes in the tetragonal space group *P*4(2)/*mnm*, and possesses a 2-D framework with square, rectangular, and rhombohedral apertures (Figure 1). The local coordination geometry around each Cd^{II} center in **1** can be described as distorted trigonal prismatic (Figure 2), in which each Cd^{II} center is coordinated by four O atoms from the chelating carboxyl groups of two bpdc ligands and two N atoms from another two bpdc ligands to complete the coordination sphere. With its two chelating carboxyl groups and bridging 2,2′-pyridyl moiety (the dihedral angle of two pyridine rings being 93.7°), each bpdc is simultaneously bound to four Cd atoms (Scheme 1), resulting in the formation of a 2-D network with three different shaped apertures. To the best of our knowledge, the four-connecting hexadentate coordination pattern of bpdc is the first such example of its kind. The architecture of **1** with the 2,2′-bipyridyl moiety bridging divalent metal centers has rarely been reported.[18−22]

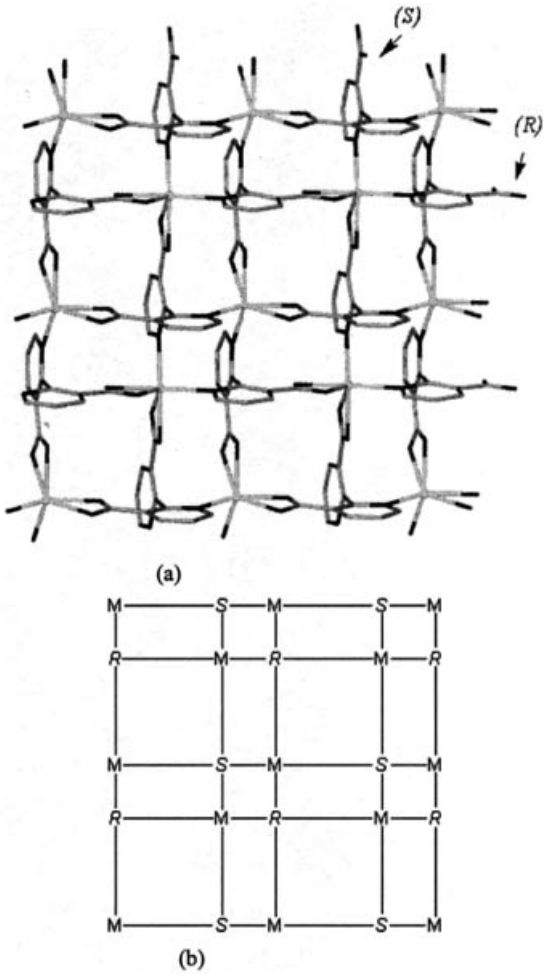

Figure 1. (a) 2-D three-shaped grid network representation of **1** (viewed along the *c* axis); (b) a simplified scheme indicating the construction of **1** interweaved by -*R*-M-*R*- and -*S*-M-*S*- chains [*R* = (*R*)-bpdc, *S* = (*S*)-bpdc and M = Cd^{II}]

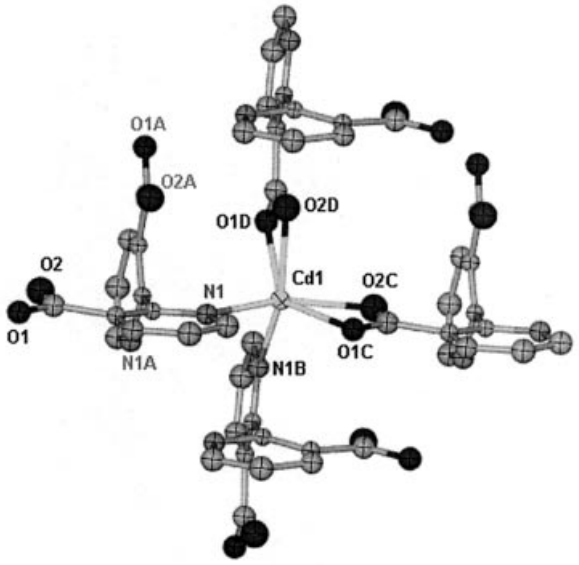

Figure 2. An ORTEP representation of the local geometry around the Cd^{II} center in **1** (50% probability thermal ellipsoids)

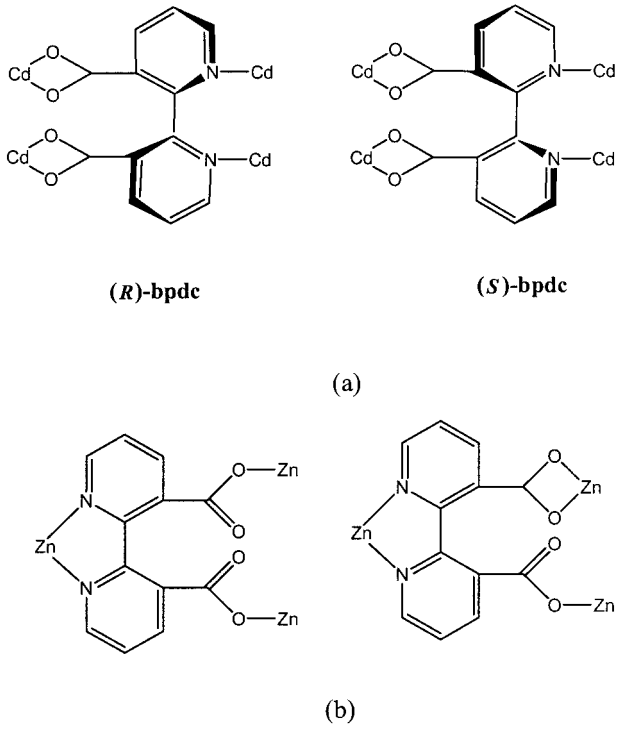

Scheme 1. Coordination modes of bpdc in (a) complex **1** and (b) complex **2**

Table 1. Selected bond lengths (Å) and angles (°) for **1** and **2**

Complex **1**

Cd1−O1C	2.399(14)	Cd1−O2C	2.305(12)
Cd1−O1D	2.399(14)	Cd1−O2D	2.305(12)
Cd1−N1	2.332(18)	Cd1−N1B	2.332(18)
O2D−Cd1−O2C	93.8(7)	O2D−Cd1−N1B	147.9(4)
O2C−Cd1−N1B	92.2(5)	O2D−Cd1−N1	92.2(5)
O2C−Cd1−N1	147.9(4)	N1B−Cd1−N1	99.1(9)
O2D−Cd1−O1C	95.8(4)	O2C−Cd1−O1C	51.4(4)
N1B−Cd1−O1C	112.4(6)	N1−Cd1−O1C	96.7(6)
O2D−Cd1−O1D	51.4(4)	O2C−Cd1−O1D	95.8(4)
N1B−Cd1−O1D	96.7(6)	N1−Cd1−O1D	112.4(6)
O1C−Cd1−O1D	134.9(8)		

Complex **2**

Zn1−O21A	1.995(6)	Zn1−O15B	2.019(6)
Zn1−O33	2.107(6)	Zn1−N2	2.115(7)
Zn1−N1	2.133(8)	Zn2−O9	1.989(6)
Zn2−O4	2.005(6)	Zn2−N4	2.108(7)
Zn2−O34	2.130(6)	Zn2−N3	2.179(7)
Zn3−O24C	2.008(6)	Zn3−N6	2.087(7)
Zn3−O35	2.094(6)	Zn3−O13	2.132(7)
Zn4−O2	1.956(6)	Zn4−O11	2.009(6)
Zn4−N16	2.088(7)	Zn4−O36	2.165(6)
Zn5−O8D	2.074(8)	Zn5−N14	2.101(8)
Zn5−O37	2.124(6)	Zn5−N13	2.125(7)
Zn6−O28	1.994(6)	Zn6−O17	2.015(6)
Zn6−O38	2.097(6)	Zn6−N8	2.117(7)
Zn6−N7	2.171(7)	Zn7−O31E	1.991(6)
Zn7−O6F	2.004(6)	Zn7−O39	2.063(7)
Zn7−N10	2.077(8)	Zn7−N9	2.178(7)
Zn8−O26	1.963(6)	Zn8−O20	1.995(6)
Zn8−N12	2.104(7)	Zn8−O40	2.139(6)
Zn8−N11	2.189(7)		
O21A−Zn1−O15B	102.3(3)	O21A−Zn1−O33	93.0(3)
O15B−Zn1−O33	97.7(3)	O21A−Zn1−N2	114.4(3)
O15B−Zn1−N2	141.2(3)	O33−Zn1−N2	92.9(3)
O21A−Zn1−N1	92.6(3)	O15B−Zn1−N1	90.3(3)
O33−Zn1−N1	169.0(3)	N2−Zn1−N1	76.2(3)
O9−Zn2−O4	118.5(3)	O9−Zn2−N4	115.4(3)
O4−Zn2−N4	126.0(3)	O9−Zn2−O34	87.4(2)
O4−Zn2−O34	93.1(2)	N4−Zn2−O34	88.3(2)
O9−Zn2−N3	105.9(3)	O4−Zn2−N3	90.6(3)
N4−Zn2−N3	75.7(2)	O34−Zn2−N3	162.4(2)
O24C−Zn3−N6	112.1(3)	O24C−Zn3−O35	95.4(3)
N6−Zn3−O35	94.4(3)	O24C−Zn3−O13	145.1(4)
N6−Zn3−O13	102.4(3)	O35)Zn3−O13	86.6(3)
O24C−Zn3−N5	83.9(3)	N6−Zn3−N5	77.0(3)
O35−Zn3−N5	170.3(3)	O13−Zn3−N5	99.6(3)
O24C−Zn3−O14	88.7(3)	N6−Zn3−O14	150.5(3)
O35−Zn3−O14	104.6(3)	O13−Zn3−O14	57.4(3)
N5−Zn3−O14	85.2(3)	O2−Zn4−O11	116.6(3)
O2−Zn4−N16	105.9(3)	O11−Zn4−N16	137.0(3)
O2−Zn4−O36	93.1(3)	O11−Zn4−O36	90.6(2)
N16−Zn4−O36	93.2(3)	O2−Zn4−N15	103.8(3)
O11−Zn4−N15	86.7(3)	N16−Zn4−N15	77.0(3)
O36−Zn4−N15	162.2(3)	O29−Zn5−O8D	141.8(4)
O29−Zn5−N14	110.5(3)	O8D−Zn5−N14	107.7(4)
O29−Zn5−O37	92.2(2)	O8D−Zn5−O37	84.6(3)
N14−Zn5−O37	94.1(3)	O29−Zn5−N13	93.0(3)
O8D−Zn5−N13	96.3(3)	N14−Zn5−N13	76.2(3)
O37−Zn5−N13	170.1(3)	O28−Zn6−O17	124.3(3)
O28−Zn6−O38	92.8(3)	O17−Zn6−O38	88.5(3)
O28−Zn6−N8	120.4(3)	O17−Zn6−N8	115.2(3)
O38−Zn6−N8	91.1(3)	O28−Zn6−N7	92.3(3)
O17−Zn6−N7	99.1(3)	O38−Zn6−N7	166.3(3)
N8−Zn6−N7	75.3(3)	O31E−Zn7−O6F	101.1(3)
O31E−Zn7−O39	97.5(3)	O6F−Zn7−O39	98.1(3)
O31E−Zn7−N10	116.5(3)	O6F−Zn7−N10	139.0(3)
O39−Zn7−N10	92.5(3)	O31E−Zn7−N9	85.9(3)
O6F−Zn7−N9	91.1(3)	O39−Zn7−N9	169.3(3)
N10−Zn7−N9	77.0(3)	O26−Zn8−O20	110.5(3)
O26−Zn8−N12	107.2(3)	O20−Zn8−N12	142.0(3)
O26−Zn8−O40	91.1(3)	O20−Zn8−O40	92.7(3)
N12−Zn8−O40	91.5(3)	O26−Zn8−N11	107.8(3)
O20−Zn8−N11	87.2(3)	N12−Zn8−N11	76.6(2)
O40−Zn8−N11	159.8(3)		

Symmetry codes: $A = 1 - y, 1 - x, 1 - z$; $B = y, x, 1 - z$; $C = x, y - 1, z$; $D = y - 1, x, 1 - z$ for 1; $A = x - 1, y + 1, z$; $B = x - 1, y, z$; $C = x, y + 1, z$; $D = x, y - 1, z$; $E = x + 1, y, z$; $F = x + 1, y - 1, z$ for 2.

The most interesting feature of **1** is that the achiral free H_2bpdc itself induces axial chirality upon metal coordination. Bpdc links to four metal centers, and exhibits a stereoselective configuration. As shown in Scheme 1, the deprotonated bpdc anions in complex **1** may exhibit (*R*) or (*S*) configurations. Each cadmium(II) center is ligated by two (*R*)-bpdc and two (*S*)-bpdc ligands. Unusually, ligands of the same configuration combine with metal nodes in the same line, so that the 2-D network is interweaved by -(*R*)-bpdc-Cd^{II}-(*R*)-bpdc- and -(*S*)-bpdc-Cd^{II}-(*S*)-bpdc- chains, as shown in Figure 1. Thus, the formation of the framework in **1** is a typical example of a metal-directed stereoselective supramolecular assembly.

In contrast to **1**, complex **2** crystallizes in the monoclinic space group *Pc*, and each asymmetric unit consists of 8 Zn^{II}, 8 bpdc, 8 H_2O, and 8 lattice H_2O units. There are two kinds of coordination geometries around the zinc(II) centers as shown in Figure 3. The Zn3 site exhibits a distorted octahedral geometry, which is surrounded by two nitrogen atoms from a bpdc bipyridyl group, four oxygen atoms from a bpdc monodentate carboxylate group, a bpdc chelating carboxylate group, and a water molecule. In contrast, the other zinc(II) centers, except for the slight difference in bond lengths and angles listed in Table 1, exhibit distorted trigonal bipyramidal environments each of which are surrounded by two nitrogen atoms from a bpdc bipyridyl group, three oxygen atoms from two other bpdc monodentate carboxylate groups, and a water molecule. The Zn−N and Zn−O distances are in the range of 2.077(8)−2.202(7) and 1.963(6)−2.443(10) Å, respectively. Unlike the four-connecting hexadentate pattern in complex **1**, each bpdc anion in complex **2** links three Zn^{II} centers with its chelating 2,2′-pyridyl moiety, asymmetrically chelating monodentate carboxyl groups, or its chelating 2,2′-pyridyl moiety and two monodentate carboxyl groups, displaying pentadentate or tetradentate three-connecting coordination modes

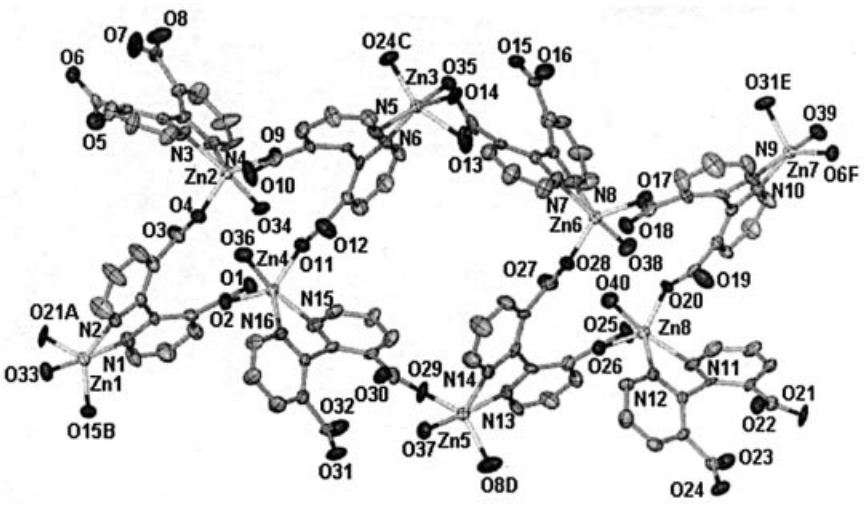

Figure 3. An ORTEP representation of the coordination geometry around the Zn^{II} centers in **2** (50% probability thermal ellipsoids); the solvent water molecules and hydrogen atoms have been omitted for clarity

due to the different coordination patterns of its carboxyl groups (see Scheme 1). The eight bpdc anions in the same asymmetric unit exhibit different distortions of the 2,2′-bipyridyl moiety along the 1,1′ bond, and the dihedral angles between their two pyridine rings are in the range of 30−45°.

The 2-D polymeric structure of **2** can be depicted as a porous grid topology. As shown in Figure 4, two triangular bpdc ligands coordinate to two Zn^{II} nodes with their carboxyl arms to form a rhombus, and further connect to Zn^{II} nodes of adjacent rhombuses with their 2,2′-bipyridyl moieties, resulting in an extended sheet along the *ab*-plane. Furthermore, cage-like pores with a diameter of about 1.2 nm are created through this regular combination of rhombuses. Through the face-to-face packing of 2-D grid sheets along *c*-axis, these cage-like pores run through each other and result in 1-D hydrophilic channels (Figure 5), where the guest water molecules reside. To the best of our knowledge, the framework architectures and unusual coordination modes of bpdc in **1** and **2** are new in the family of bpdc-containing complexes.

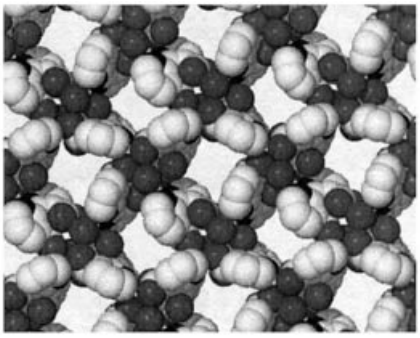

Figure 5. View of the 1-D hydrophilic tunnels along the *c* axis in **2** (guest water molecules have been omitted for clarity)

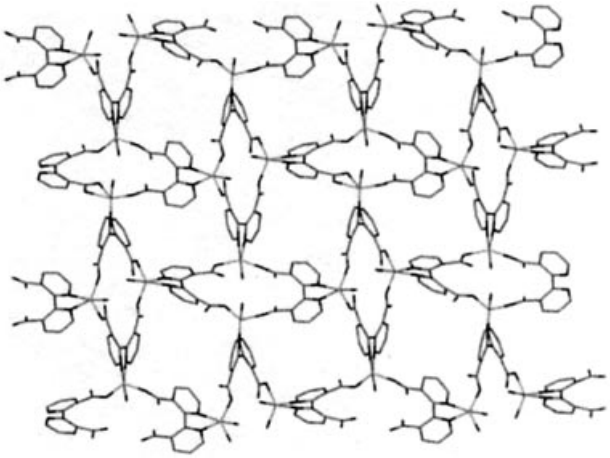

Figure 4. Perspective view of the 2-D network with square cavities and rhombuses in **2**

Fluorescence Properties

Investigations of the solid emissions of Me_2bpdc, **1**, and **2** indicate, that the intraligand fluorescence emission (IL) wavelength and intensity can be tuned by altering the configuration of bpdc, i.e. the dihedral angle between its pyridine moieties. The emissions of **1** [$\lambda_{max.}$ = 404 nm] and **2** [$\lambda_{max.}$ = 448 nm] can be tentatively assigned to the intraligand fluorescence emission, since a similar but weaker emission [$\lambda_{max.}$ = 443 nm for Me_2bpdc] can also be observed for the free ligand (Figure 6). Generally, the intraligand fluorescence emission wavelength of a multi-pyridine ligand is determined by the energy gap between the π and π* molecular orbitals of the free ligand, which is simply related to the extent of π conjugation in the system. For bpdc, however, whose 2,2′-bipyridyl moiety can rotate along the 1,1′ bond, the π and π* energy levels may be perturbed by the dihedral angle between the pyridine rings according to Perkovic's hy-

pothesis.[23] The unexpected blue-shifted emission of **1** and the slightly red-shifted emission of **2** have been examined. As the dihedral angle of the 2,2′-bipyridyl moiety changes from 53.2° in Me_2bpdc to 93.7° in bpdc in complex **1**,[26] the energy gap between the π* and π molecular orbitals of bpdc increases. Thus, the maximum emission wavelength of **1** undergoes a blue-shift. However, as the dihedral angle of the 2,2′-bipyridyl moiety in **2** decreases to around 30−45°, the energy gap between the π* and π molecular orbitals of bpdc decreases, and the maximum emission wavelength of **2** undergoes a red-shift. The emission intensities of **1** and **2** increase relative to that of Me_2bpdc, and are approximately 1.6 and 1.3 times larger than that of Me_2bpdc, respectively. These enhancements perhaps result from the coordination of bpdc to Cd^{II} or Zn^{II}, which increases the conformational rigidity of the ligands, therefore reducing the non-radiative decay of the intraligand $^1(\pi$-$\pi^*)$ excited state. Similar enhancements of the intraligand fluorescence have also been found in polypyridyl cadmium(II) and polypyridyl zinc(II)polymers.[27−30]

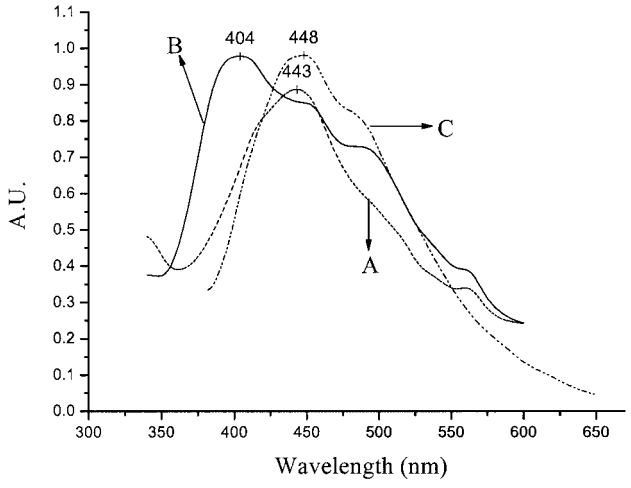

Figure 6. Fluorescence spectra of Me_2bpdc (A), **1** (B), and **2** (C) in the solid state at room temperature (the height of curve A has been reduced for clarity)

Conclusion

Based on the alteration of the configuration of bpdc induced by metal centers, two new 2-D coordination polymers have been obtained by self-assembly of bpdc with Cd^{II} or Zn^{II}. The achiral free H_2bpdc itself causes axial chirality by upon metal coordination in **1**, while in **2** it displays a different distortion of the 2,2′-bipyridyl moiety along the 1,1′ bond to meet the requirements of the final structural motif. Through tuning the configuration of bpdc, complexes **1** and **2** display stronger fluorescence emissions at different wavelengths, which may result in their exploitation in photo-materials.

Experimental Section

General Remarks: Except for binicotinic acid and dimethyl 2,2′-bipyridine-3,3′-dicarboxylate, which were synthesized by literature methods,[31] all other materials were used as received. The IR spectra in KBr disk were recorded with a Magna 750 FT-IR spectrophotometer. C, H and N elemental analyses were determined with an Elementary Vario ELIII elemental analyzer. Fluorescence spectra were measured with an Edinburgh FL-FS90 TCSPC system.

$[Cd^{II}(bpdc)]_n$ (1): Hydrothermal treatment of $CdCl_2{\cdot}2.5H_2O$ (0.2 mmol), Me_2bpdc (0.2 mmol), triethylamine (0.1 mL), and water (15 mL) at 160 °C for 5 days yielded colorless, crystalline blocks of **1** with only one pure phase. The yield of **1** was 55%. $C_{12}H_6CdN_2O_4$ (354.6): calcd. C 40.68, H 1.69, N 7.91; found C 41.10, H 1.44, N 7.91. IR (KBr): $\tilde{\nu}$ = 3093 cm^{-1} (w), 1616 (s), 1577 (s), 1566 (s), 1493 (sh, w), 1431 (m), 1400 (s), 1157 (m), 874 (m), 796 (s), 434 (m).

$\{[Zn^{II}_8(bpdc)_8(H_2O)_8](H_2O)_8\}_n$ (2): With a solution of H_2bpdc (0.2 mmol) in water (20 mL) as the bottom layer in a 50-mL tube, a mixture of water (5 mL), methanol (5 mL), and DMF (10 mL) was added dropwise to the tube along its wall to form a middle layer. A solution of $ZnCl_2$ (0.2 mmol) in methanol (10 mL) was then added as the top layer. After slowly diffusing for two weeks, colorless blocks of **2** appeared in the mesosphere and the yield of **2** was 40%. $C_{96}H_{80}N_{16}O_{48}Zn_8$ (2748.72): calcd. C 41.95, H 2.93, N 8.15; found C 41.70, H 2.84, N 8.18. IR (KBr): $\tilde{\nu}$ = 3461 cm^{-1} (br., s), 3096 (w), 3004 (w), 1653 (s), 1616 (s), 1582 (s), 1432 (m), 1381 (vs), 1161 (m), 1115 (w), 874 (m), 786 (s), 447 (m).

X-ray Crystallographic Determinations: A prismatic crystal of complex **1** with approximate dimensions of 0.46 × 0.28 × 0.04 mm, and a block crystal of complex **2** with approximate dimensions of 0.33 × 0.16 × 0.10 mm, respectively, were selected for X-ray diffraction analysis. The unit-cell parameters and intensities were collected at 298(2) K on a Siemens SMART CCD diffractometer with graphite-monochromated Mo-K_α radiation (λ = 0.71073Å) using the ω-scan mode. The structures were solved by direct methods, and refined on F^2 by full-matrix least-squares procedures using the SHELXTL software suite.[32] All non-hydrogen atoms were refined anisotropically. For complex **1**, no hydrogen atoms were theoretically located, and the maximum and minimum peaks in the final difference maps were 2.211 and −1.573 e·$Å^{-3}$ due to the statistical distribution of the pyridine rings. The largest residual density peak is close to the carboxyl group. For complex **2**, the positions of the hydrogen atoms in the pyridine rings were generated geometrically, and the maximum and minimum peaks in the final difference maps were 1.188 and −0.397 e·$Å^{-3}$ from the disordered solvent water molecule, respectively. The Flack x parameter of complex **2** is 0.3200 with an esd 0.0120 before a twin model refinement, and its absolute structural parameter is 0.00 in the final list of crystal and structural refinement data for complex **2**. A summary of the crystallographic data of complexes **1** and **2** is presented in Table 2, and their selected bond lengths and bond angles are listed in Table 1. CCDC-217300 and CCDC-223662 contain the supplementary crystallographic data for **1** and **2**, respectively. These data can be obtained free of charge at www.ccdc.cam.ac.uk/conts/retrieving.html [or from the Cambridge Crystallographic Data Center, 12 Union Road, Cambridge CB2 1EZ, UK; Fax: (internat.) + 44-1223-336-033; E-mail: deposit@ccdc.cam.ac.uk].

Acknowledgments

This work was supported by grants from the National Natural Science Foundation of China (No.20231020) and the Natural Science Foundation of Fujian Province.

Table 2. Crystal data and refinement data for **1** and **2**

	1	**2**
Empirical formula	$C_{12}H_6CdN_2O_4$	$C_{96}H_{80}N_{16}O_{48}Zn_8$
Molecular mass	354.6	2748.72
Temperature (K)	298(2)	298(2)
Wavelength (Å)	0.71073	0.71073
Crystal system, space group	tetragonal, *P*4(2)/*mnm*	monoclinic, *Pc*
a (Å)	8.1884(9)	19.6871(10)
b (Å)	8.1884(9)	19.761(0)
c (Å)	16.432(3)	15.543(0)
α (°)	90	90
β (°)	90	101.973(2)
γ (°)	90	90
V (A^3)	1101.8(2)	5915.5(3)
Z, $\rho_{calcd.}$ (Mg m^{-3})	16, 2.101	2, 1.543
μ (Mo-K_α) (mm^{-1})	1.992	1.687
F(000)	664	2784
θ range (°)	2.78 to 25.03	3.05 to 22.50
Reflections collected/unique	2444/ 557 [*R*(int) = 0.0522]	28583/13398 [*R*(int) = 0.0310]
Goodness-of-fit on F^2	1.316	1.076
*R*1, *wR* [$I > 2\sigma(I)$] (all data)	0.0630, 0.1790, 0.0753, 0.1864	0.0497, 0.1320, 0.0535, 0.1356

[1] O. Kahn, C. J. Martinez, *Science* **1998**, *279*, 44−48.
[2] O. Kahn, *Acc. Chem. Res.* **2000**, *33*, 647−657.
[3] O. M. Yaji, G. M. Li, *Angew. Chem. Int. Ed. Engl.* **1995**, *34*, 207−209.
[4] J. S. Seo, D. Whang, H. Lee, S. I. Jun, J. Oh, Y. J. Jeon, K. Kim, *Nature* **2000**, *404*, 982−986.
[5] W.-B. Lin, O. R. Evans, R.-G. Xiong, Z.-Y. Wang, *J. Am. Chem. Soc.* **1998**, *120*, 13272−13273.
[6] J. Zhang, Y.-R. Xie, Q. Ye, R.-G. Xiong, Z. Xue, X.-Z. You, *Eur. J. Inorg. Chem.* **2003**, 2572−2577.
[7] L. C. Tabares, J. A. R. Navarro, J. M. Salas, *J. Am. Chem. Soc.* **2001**, *123*, 383−387.
[8] O. M. Yaghi, H. Li, *J. Am. Chem. Soc.* **1996**, *118*, 295−296.
[9] O. M. Yaghi, H. Li, T. L. Groy, *J. Am. Chem. Soc.* **1996**, *118*, 9096−9101.
[10] O. R. Evans, W. Lin, *Inorg. Chem.* **2000**, *39*, 2189−2198.
[11] P. Ayyappan, O. R. Evans, W. Lin, *Inorg. Chem.* **2002**, *41*, 3328−3330.
[12] K. Biradha, M. Fujita, *Chem. Commun.* **2001**, 15−16.
[13] J. Kim, B. Chen, T. M. Reineke, H. Li, M. Eddaoudi, D. B. Moler, M. O'keeffe, O. M. Yaghi, *J. Am. Chem. Soc.* **2001**, *123*, 8239−8247.
[14] K. Seki, *Chem. Commun.* **2001**, 1496−1497.
[15] C. J. Kepert, M. J. Rosseinsky, *Chem. Commun.* **1998**, 31−32.
[16] M. Eddaoudi, H. Li, O. M. Yaghi, *J. Am. Chem. Soc.* **2000**, *122*, 1391−1397.
[17] Y.-H. Liu, Y.-L. Lu, H.-Ch. Wu, J.-Ch. Wang, K.-L. Lu, *Inorg. Chem.* **2002**, *41*, 2592−2597.
[18] G. Y. S. K. Swamy, K. Chandramohan, N. V. Lakshmi, K. Ravikumar, *Z. Kristallogr.* **1998**, *213*, 191−194.
[19] Zh. J. Zhong, X.-Z. You, Q.-CH. Yang, *Polyhedron* **1994**, *13*, 1951−1955.
[20] X.-M. Zhang, H.-Sh. Wu, X.-M. Chen, *Eur. J. Inorg. Chem.* **2003**, 2959−2964.
[21] B.-L. Wu, H.-Q. Zhang, H.-Y. Zhang, Q.-A. Wu, H.-W. Hou, Y. Zhu, X.-Y. Wang, *Aust. J. Chem.* **2003**, *56*, 335−338.
[22] M.-L. Tong, G. Yang, X.-M. Chen, *Aust. J. Chem.* **2000**, *53*, 607−610.
[23] M. W. Perkovic, *Inorg. Chem.* **2000**, *39*, 4962−4968.
[24] P.-X. Xie, Y.-J. How, B.-W. Zhang, F. Wu, W.-J. Tian, J.-C. Shen, *J. Chem. Soc., Dalton Trans.* **1999**, 4217−4221.
[25] S. Menon, M. V. Rajasekharan, J. P. Tuchagues, *Inorg. Chem.* **1997**, *36*, 4341−4346.
[26] C. R. Rice, K. J. Robinson, J. D. Wallis, *Acta Crystallogr., Sect. C* **1993**, *49*, 1980−1982.
[27] Ch.-G. Zheng, Y.-L. Xie, R.-G. Xiong, X.-Z. You, *Inorg. Chem. Commun.* **2001**, *4*, 405−408.
[28] J. Zhang, Y.-R. Xie, Q. Ye, R.-G. Xiong, Z.-L. Xue, X.-Z. You, *Eur. J. Inorg. Chem.* **2003**, 2572−2577.
[29] J.-H. Luo, M.-Ch. Hong, R.-H. Wang, R. Cao, L. Han, Zh.-Zh. Lin, *Eur. J. Inorg. Chem.* **2003**, 2705−2710.
[30] L. Han, M.-C. Hong, R.-H. Wang, J.-H. Luo, Zh.-Zh. Lin, D.-Q. Yuan, *Chem. Commun.* **2003**, 2580−2581.
[31] S. Dholakia, R. D. Gillard, F. l. Wimmer, *Polyhedron* **1985**, *4*, 791−795.
[32] G. M. Sheldrick, Bruker SHELXTL-PC, University of Göttingen, Germany, **1997**.

Received December 1, 2003
Early View Article
Published Online May 5, 2004

